Int J Fract (2019) 215:77–89
https://doi.org/10.1007/s10704-018-00335-9

ORIGINAL PAPER

Finite strain theory of a Mode III crack in a rate dependent gel consisting of chemical and physical cross-links

Chung Yuen Hui · Jingyi Guo · Mincong Liu · Alan Zehnder

Received: 2 June 2018 / Accepted: 27 November 2018 / Published online: 3 January 2019

Abstract In previous works we developed a three-dimensional large deformation constitutive theory for a dual cross-link hydrogel gel with permanent and transient bonds. This theory connects the breaking and reforming kinetics of the transient bonds to the nonlinear elasticity of the gel network. We have shown that this theory agrees well with experimental data from both tension and torsion tests. Here we study the mechanics of a Mode *III or* anti-plane shear crack for this particular class of rate dependent solids. We first show that our constitutive model admits a non-trivial state of anti-plane shear deformation. We then establish a correspondence principle for the special case where the chains in the network obey Gaussian statistics. For this special case there is a one to one analogy between our model and standard linear viscoelasticity. We also study the asymptotic behavior of the time dependent crack tip field, and show that for a wide class of network energy density functions, the *spatial* singularities of these fields are identical to a hyper-elastic, cracked body with the same but undamaged networks.

Keywords Self-healing hydrogel · Mode III crack · Asymptotics · Rate dependence · Correspondence principle

C. Y. Hui (✉) · J. Guo · M. Liu · A. Zehnder
Field of Theoretical and Applied Mechanics, Department of Mechanical and Aerospace Engineering, Cornell University, Ithaca, NY 14583, USA
e-mail: ch45@cornell.edu

1 Introduction

A hydrogel is a network of polymer chains swollen in water. Due to the large water content, they can be highly compliant (with shear moduli ranging from a few Pa to 100 kPa), bio-compatible and exhibit low friction, making them ideal candidates for many bio-engineering applications such as scaffolds for cells in tissue engineering (Kuo and Ma 2001; Lee and Mooney 2001), artificial cartilage (Kwon et al. 2014) and vehicles for drug delivery (Qiu and Park 2001). However, the high water content of these gels also limits their use as structural materials since they have very low resistance to fracture. There have been rapid advances in this field since 2003, when Gong et al. (2003) synthesized a highly extensible double network (DN) hydrogel with fracture toughness $\sim 10^3$ J/m^2, comparable to that of synthetic rubber. This gel consists of two interpenetrating networks: the first network is tightly cross-linked and swollen while the second network is loosely cross-linked and highly extensible (Gong et al. 2003; Webber et al. 2007). When subjected to mechanical loading, the first network bears most of the load and undergoes progressive damage and the second extensible network prevents the formation and growth of macroscopic cracks (Brown 2007; Gong 2010; Nakajima et al. 2013; Wang and Hong 2011). More recently, several research groups (Henderson et al. 2010; Lin et al. 2010; Mayumi et al. 2013; Narita et al. 2013; Sun et al. 2012, 2013) have found that highly stretchable

and tough hydrogels can also be made by replacing the covalent bonds in the stiff network by temporary physical bonds. Since physical bonds can reform after breakage, upon unloading and resting, these DN gels can partially or fully recover to their original state depending on the resting period. Due to the kinetics of the physical bonds, these self-healing gels exhibit time dependent behavior similar to nonlinear viscoelastic solids (Lin et al. 2010; Mayumi et al. 2013; Narita et al. 2013; Sun et al. 2012, 2013).

There are many open questions on the rate dependent mechanical behavior of these gels. Until our recent works (Long et al. 2014, 2015) there have been no quantitative constitutive descriptions for the large strain time dependent behavior of these gels. In these works (Long et al. 2014, 2015) we studied the mechanical behavior of a poly(vinylalcohol) (PVA) dual crosslinked gel with PVA chemically crosslinked by glutaraldehyde and physically crosslinked by Borax ions (Mayumi et al. 2013; Narita et al. 2013). Although this gel has lower resistance to fracture in comparison to the polyampholyte gel developed by Sun et al. (2013), it has a well-defined simple chemical structure with only one type of physical crosslink between PVA chains. As a result, in linear rheology tests, the loss modulus has a well-defined relaxation time. In addition, the dynamics of bond breaking and healing are found *experimentally to be nearly independent of strain over a wide range of strain amplitude, which is typically not the case for more complex gels*. From this perspective it serves a model system to study the interplay between bond kinetics and macroscopic mechanical behavior of the hydrogel having transient crosslinks. In several papers (Guo et al. 2016; Long et al. 2014, 2015), we have shown that a three-dimensional constitutive model which combines the finite strain elasticity of the networks with the kinetics of bond breaking and reattachment can accurately predict the behavior of uni-axial tension and torsion tests with *complex* loading histories.

Although there have been some experimental studies on the fracture behavior of these self-healing gels (Mayumi et al. 2016), we are not aware of any quantitative analyses of their fracture mechanics. This is because these gels are often subjected to very large deformation; the nonlinearity due to finite strain kinematics and material behavior as well as *history dependence* make quantitative analysis extremely difficult. Our aim is to provide such an analysis, albeit for the simple case of Mode *III* or anti-plane shear fracture. The kinematic simplicity of Mode III fracture allows us to reduce the mathematical complexities associated with plane strain or plane stress cracks and to gain insight into the mechanics of fracture in more complex geometries. For example, Rice studied the stresses due to sharp notches in elastic–plastic solids loaded in anti-plane shear using the hodograph technique (Rice 1967), Chitaley and McClintock (1971) studied the plastic deformation of a steady state growing crack under anti-plane shear. More recently, Long and Hui studied the effect of finite chain extensibility on the stress and strains near the tip of Mode III crack (Long and Hui 2015).

Many previous works use a linearized version of anti-plane shear which assumes small deformation. As noted by the seminal work of Knowles (1977), only a certain class of *hyper-elastic* incompressible solids admits a non-trivial state of anti-plane shear deformation. Since our constitutive model is nonlinear viscoelastic, it is not clear that it admits a non-trivial state of anti-plane shear deformation. The proof that it indeed does and a brief review of our constitutive model are given in Sects. 2 and 3 of this paper. In Sect. 4, we studied several special cases which lends insight to the time dependent deformation and stress fields in these gels. Summary and discussion is given in Sect. 4.

2 Review of constitutive model

We briefly review our constitutive model. Details can be found in our previous works (Guo et al. 2016; Long et al. 2014). Macroscopically the gel is assumed to be isotropic and incompressible. It consists of two independent networks: the chemical crosslinks form a permanent elastic network and the physical crosslinks form a transient elastic network that can break and reattach with rates independent of the stress or strain acting on it. We assume the chemical cross-links do not break. Further, when a polymer chain in the transient network breaks, it instantaneously releases the strain energy it carries. Also, when a broken chain reattaches at time τ, it has zero strain energy at that time, even though the transient network is under stress. The deformation of temporary chains reconnected at time τ is described by the deformation gradient tensor $\mathbf{F}^{\tau\to t}$. The superscript $\tau \to t$ indicates that the temporary chain experiences the deformation history from its birth (reattachment)

at τ to the current time t. The total strain energy is equal to the sum of the strain energy carried by each chain in both networks and is given by an energy density function. Although not necessary, we assume the strain energy densities of the *undamaged* networks are the same; denoted by W, a function *only* of the strain invariant $I_1 \equiv tr\left[\mathbf{F}^{\mathrm{T}}\mathbf{F}\right]$, where $\mathbf{F}$ is the deformation gradient. We also assume the breaking and reattaching of the physical chains reaches a dynamic equilibrium soon after the gel is synthesized. This steady state assumption implies that the breaking and reattachment rates are equal and independent of time. These rates are denoted by $\bar{\gamma}_\infty$.

Without loss of generality, we assume loading commences at $t = 0$ and prior to that no mechanical loading has ever been applied. With these assumptions, the nominal stress tensor $\mathbf{P}$ is related to the deformation gradient $\mathbf{F}^{\tau\to t}$ by

$$\begin{aligned}\mathbf{P} = &-p\left(\mathbf{F}^{0\to t}\right)^{-\mathrm{T}} + 2\left[n(t)+\rho\right] W'(I_1)\big|_{I_1=H(0,t)} \\ &\times \mathbf{F}^{0\to t} + 2\bar{\gamma}_\infty \int_0^t \phi_B\left(\frac{t-\tau}{t_B}\right) W'(I_1)\big|_{I_1=H(\tau,t)} \\ &\times \mathbf{F}^{\tau\to t}\left(\mathbf{F}^{0\to\tau}\right)^{-\mathrm{T}} d\tau \end{aligned} \tag{1a}$$

where $W'(I_1) = dW/dI_1$ and

- p is the Lagrange multiplier which enforces incompressibility,
- ρ is the molar fraction of the chemical crosslinks,
- In the integral term of (1a), $W'(I_1)$ is evaluated at $I_1 = H(x,\tau,t) \equiv tr\left[\left(\mathbf{F}^{\tau\to t}\right)^{\mathrm{T}}\mathbf{F}^{\tau\to t}\right]$ to account for the fact that the strain energy carried by temporary chains that are reattached at τ and survive to the current time t depends only on the deformation during this period of time.
- $$\begin{aligned}&\phi_B\left((t-\tau)/t_B\right) \\ &= \left[1+(\alpha_B-1)(t-\tau)/t_B\right]^{1/(1-\alpha_B)}\end{aligned} \tag{1b}$$

is the "survivability" function, the fraction of physical crosslinks that are formed at time τ and remain attached at time $t \geq \tau$. Here t_B is the characteristic time for breaking and $1 < \alpha_B < 2$ is a material parameter. Physically, the 2nd integral term in (1a) accounts for the forces carried by chains that reattach at different times $0 \leq \tau \leq t$ and survives to the current time t.

- $n(t)$ is the fraction of physical crosslinks that are attached at $t = 0$ and survive until current time $t \geq 0$ and is given by

$$\begin{aligned}n(t) &\equiv \bar{\gamma}_\infty \int_t^\infty \phi_B\left(\tau/t_B\right) d\tau \\ &= \bar{\gamma}_\infty \frac{t_B}{2-\alpha_B}\left[1+(\alpha_B-1)\frac{t}{t_B}\right]^{\frac{2-\alpha_B}{1-\alpha_B}}\end{aligned} \tag{1c}$$

Note that $n(t)$ is a decaying function of time since $2 > \alpha_B > 1$.

To gain physical insight, consider the special case of uniaxial tension; (1a) reduces to

$$\begin{aligned}\mathbf{P}_{11} = &\,2\left[\rho+n(t)\right] W'(I_1)\big|_{\mathrm{H}(0,t)}\left[\lambda(t)-\frac{1}{\lambda^2(t)}\right] \\ &+ 2\bar{\gamma}_\infty \int_0^t \phi_B\left(\frac{t-\tau}{t_B}\right) W'(I_1)\big|_{H(\tau,t)} \\ &\times\left[\frac{\lambda(t)}{\lambda^2(\tau)}-\frac{\lambda(\tau)}{\lambda^2(t)}\right] d\tau\end{aligned} \tag{1d}$$

where $\mathbf{P}_{11}$ is the nominal stress and λ is the stretch ratio in the loading direction, and

$$\begin{aligned}I_1(t) &= \lambda^2(t) + \frac{2}{\lambda(t)}, \\ H(\tau,t) &= \left[\lambda(t)/\lambda(\tau)\right]^2 \\ &\quad + 2\lambda(\tau)/\lambda(t),\ \tau < t,\end{aligned} \tag{1e}$$

The first term on the right hand side of (1d) describes the loss of stress due to breaking of the original temporary strands while the integral term describes the recovery of stress from the reattachment of temporary strands.

In our previous works (Guo et al. 2016; Long et al. 2014, 2015), we have demonstrated that our model can accurately predict the mechanical behavior of the PVA dual-crosslink hydrogel subjected to complex loading histories. Figure 1 highlights some recent data on cyclic test where a uniaxial tension specimen is first loaded at a certain stretch rate, then unloaded at a different stretch rate. The solid lines are experimental data and the dotted lines are obtained using our model using material parameters determined separately from relaxation tests. Since the focus of this work is on crack tip fields, details of experimental procedures and fitting methods will not be repeated here. More data including rheology and torsion tests can be found in Guo et al. (2016) and Long et al. (2014, 2015).

3 Existence of anti-plane shear deformation

Our proof follows the approach of Knowles (1977). As noted by Knowles: "A solid which occupies a cylindri-

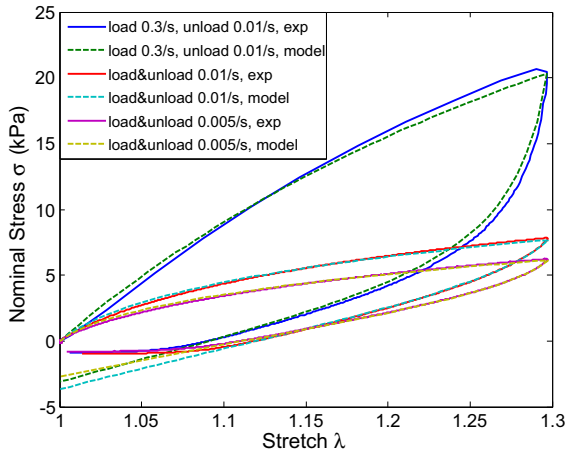

Fig. 1 Experimental results and model prediction of the stress-stretch behavior of one PVA dual-crosslink hydrogel sample in constant rate uniaxial tension tests of different loading and unloading rates. The solid curves are experimental results and the dashed curves are model predictions. The material parameters in our model are: $\mu\rho = 3.8091\,\text{kPa}$, $\mu\bar{\gamma}_\infty = 18.68\,\text{kPa/s}$, $\alpha_B = 1.6137$, $t_B = 0.6606\,\text{s}$

cal region in its undeformed configuration is said to be deformed to a state of anti-plane shear if the displacement of each material point is parallel to the generators of the cylinder (which we took to be in the direction of the unit vector $\mathbf{E}_3$) and is independent of x_3, the out of plane coordinate." We identify a material point in the undeformed reference configuration by the $2D$ vector

$$\mathbf{x} \equiv x_\alpha \mathbf{E}_\alpha \quad \alpha = 1, 2 \tag{2a}$$

Here $\{\mathbf{E}_1, \mathbf{E}_2, \mathbf{E}_3\}$ are orthonormal vectors which form a right handed basis. In the following, we used the summation convention of summing over repeated indices. Also, we assume quasi-static deformation in the absence of body forces.

By definition, the only non-vanishing displacement is $w\,(x_1, x_2, t)$ in the out of plane direction. A straight forward but tedious calculation using the definition of deformation gradient and $\mathbf{F}^{\tau\to t} = \left(\mathbf{F}^{0\to\tau}\right)^{-1}\mathbf{F}^{0\to t}$ shows that the matrices representing the tensors $\mathbf{F}^{0\to t}$ and $\mathbf{F}^{\tau\to t}\left(\mathbf{F}^{0\to\tau}\right)^{-\mathrm{T}}$ with respect to the Cartesian basis $\{\mathbf{E}_1, \mathbf{E}_2, \mathbf{E}_3\}$ are:

$$\left[\mathbf{F}^{0\to t}\right] = \begin{bmatrix} 1 & 0 & 0 \\ 0 & 1 & 0 \\ w,_1\,(\mathbf{x}, t) & w,_2\,(\mathbf{x}, t) & 1 \end{bmatrix}, \tag{2b,c}$$

$$\mathbf{F}^{\tau\to t}\left(\mathbf{F}^{0\to\tau}\right)^{-\mathrm{T}} = \begin{bmatrix} 1 & 0 & -w,_1\,(\mathbf{x}, \tau) \\ 0 & 1 & -w,_2\,(\mathbf{x}, \tau) \\ \Delta w,_1 & \Delta w,_2 & \omega_{33} \end{bmatrix}$$

where

$$w,_\alpha \equiv \partial w/\partial x_\alpha, \tag{2d–f}$$
$$\Delta w\,(\mathbf{x}, t, \tau) = w\,(\mathbf{x}, t) - w\,(\mathbf{x}, \tau) \text{ and}$$
$$\omega_{33} = 1 - w,_1\,(\mathbf{x}, \tau)\Delta w,_1 - w,_2\,(\mathbf{x}, \tau)\Delta w,_2$$

Also,

$$H\,(\mathbf{x}, 0, t) \equiv tr\left[\left(\mathbf{F}^{0\to t}\right)^{\mathrm{T}}\mathbf{F}^{0\to t}\right] = 3 + w,_\alpha\,(\mathbf{x}, t) w,_\alpha\,(\mathbf{x}, t) \tag{2g}$$

$$H\,(\mathbf{x}, \tau, t) = tr\left[\left(\mathbf{F}^{\tau\to t}\right)^{\mathrm{T}}\mathbf{F}^{\tau\to t}\right] = 3 + \Delta w,_\alpha\,(\mathbf{x}, t, \tau)\,\Delta w,_\alpha\,(\mathbf{x}, t, \tau) \tag{2h}$$

Substituting (2b–h) into (1a), the nominal stress components are:

$$P_{3\alpha} = 2\,[n(t) + \rho]\,W'\,(H_0)\,w,_\alpha + 2\bar{\gamma}_\infty \int_0^t \phi_B\left(\frac{t-\tau}{t_B}\right) W'\,(H)\,\Delta w,_\alpha\,d\tau \tag{3a}$$

$$P_{33} = -p + \left\{2\,[n(t) + \rho]\,W'\,(H_0) + 2\bar{\gamma}_\infty \int_0^t \frac{\phi_B\left(\frac{t-\tau}{t_B}\right)}{W'\,(H)\,(-w,_1\,\Delta w,_1 - w,_2\,\Delta w,_2 + 1)}\,d\tau\right\} \tag{3b}$$

$$P_{11} = P_{22} = -p + 2\,[n(t) + \rho]\,W'\,(H_0) + 2\bar{\gamma}_\infty \int_0^t \phi_B\left(\frac{t-\tau}{t_B}\right) W'\,(H)\,d\tau \tag{3c}$$

$$P_{\alpha 3} = pw,_\alpha\,(\mathbf{x}, t) - 2\bar{\gamma}_\infty \int_0^t \phi_B\left(\frac{t-\tau}{t_B}\right) W'\,(H)\,w,_\alpha\,(\mathbf{x}, \tau)\,d\tau \tag{3d}$$

$$P_{12} = P_{21} = 0 \tag{3e}$$

Since the quantity inside the curly bracket in (3b) is *independent* of x_3, the equilibrium equation in the out of plane direction $P_{3\alpha},_\alpha + P_{33},_3 = 0$ reduces to

$$p,_3 = P_{3\alpha},_\alpha = 2\,[n(t) + \rho]\left[W'\,(H_0)\,w,_\alpha\right],_\alpha + 2\bar{\gamma}_\infty \int_0^t \phi_B\left(\frac{t-\tau}{t_B}\right)\left(W'\,(H)\,\Delta w,_\alpha\right),_\alpha\,d\tau \tag{4}$$

Since the RHS of (4) is independent of x_3, p must be a linear function of x_3, that is,

$$p = \phi(\mathbf{x}, t)x_3 + c(\mathbf{x}, t) \tag{5a}$$

where

$$\phi(\mathbf{x}, t) = 2\left[n(t) + \rho\right]\left[W'(H_0)\, w_{,\alpha}\right]_{,\alpha} + 2\bar{\gamma}_\infty \int_0^t \phi_B\left(\frac{t-\tau}{t_B}\right)\left(W'(H)\,\Delta w_{,\alpha}\right)_{,\alpha}\, d\tau, \tag{5b}$$

and $c(\mathbf{x}, t)$ is an undetermined function. To determine $c(\mathbf{x}, t)$, in-plane equilibrium requires:

$$P_{11,1} + P_{13,3} = -p_{,1} + \left[2\left[n(t) + \rho\right] W'(H_0) + 2\bar{\gamma}_\infty \int_0^t \phi_B\left(\frac{t-\tau}{t_B}\right) W'(H)\, d\tau\right]_{,1} + p_{,3}\, w_{,1} = 0 \tag{6a}$$

$$P_{22,2} + P_{23,3} = -p_{,2} + \left[2\left[n(t) + \rho\right] W'(H_0) + 2\bar{\gamma}_\infty \int_0^t \phi_B\left(\frac{t-\tau}{t_B}\right) W'(H)\, d\tau\right]_{,2} + p_{,3}\, w_{,2} = 0 \tag{6b}$$

Equation (6a,b) can be rewritten as

$$\left[p - 2\left[n(t) + \rho\right] W'(H_0) + 2\bar{\gamma}_\infty \int_0^t \phi_B\left(\frac{t-\tau}{t_B}\right) W'(H)\, d\tau\right]_{,\alpha} - p_{,3}\, w_{,\alpha} = 0 \tag{7}$$

Substituting (5a) into (7) gives:

$$p_{,\alpha} = \left[2\left[n(t) + \rho\right] W'(H_0) + 2\bar{\gamma}_\infty \int_0^t \phi_B\left(\frac{t-\tau}{t_B}\right) W'(H)\, d\tau\right]_{,\alpha} + \phi(\mathbf{x}, t) w_{,\alpha} \tag{8}$$

where $H_0 = H(\mathbf{x}, 0, t)$ and we hide the arguments in H to simplify notation. Since the *RHS* of (8) is independent of x_3, $p_{,\alpha}$ *must be independent of* x_3; substituting (5a) into (8) shows that

$$\phi_{,\alpha}(\mathbf{x}, t) = 0 \Rightarrow \phi(\mathbf{x}, t) = f(t), \tag{9}$$

for some unknown $f(t)$. Equation (5a) can now be written as

$$p = f(t)x_3 + c(\mathbf{x}, t) \tag{10}$$

Substituting (10) into (8) with $\phi(\mathbf{x}, t) = f(t)$ and integrating gives:

$$c(\mathbf{x}, t) = f(t)w(\mathbf{x}, t) + 2\left[n(t) + \rho\right] W'(H_0) + 2\bar{\gamma}_\infty \int_0^t \phi_B\left(\frac{t-\tau}{t_B}\right) W'(H)\, d\tau + d(t) \tag{11}$$

where $d(t)$ is an arbitrary function of time.

To determine the functions $f(t)$ and $d(t)$, we use the fact that the crack faces are traction free for all times. Here when we assume the crack is straight and occupies a closed interval C on $x_2 = 0$, the traction free condition is:

$$P_{21} = P_{22} = P_{23} = 0 \quad \forall t \quad x_1 \in C \tag{12}$$

By (3e), $P_{21} = 0$ is automatically satisfied. Using (3d), (10) and (11), the condition $P_{22} = 0$ on the crack face is

$$-f(t)x_3 - f(t)w(\mathbf{x}, t) - d(t) = 0, \tag{13}$$

for *all times* and *all* x_3, these imply

$$f(t) = d(t) = 0 \tag{14}$$

Substituting (14) into (11) and using (10), p is

$$p = c(\mathbf{x}, t) = 2\left[n(t) + \rho\right] W'(H_0) + 2\bar{\gamma}_\infty \int_0^t \phi_B\left(\frac{t-\tau}{t_B}\right) W'(H)\, d\tau \tag{15}$$

A special case is when the chains obey Gaussian statistics, for this case W is neo-Hookean, i.e.,

$$W = \frac{\mu}{2}(I_1 - 3) \Rightarrow W' = \frac{\mu}{2} \tag{16}$$

where μ is the small strain shear modulus. Direct evaluation of the integral in (15) using (1b) and (16) results in

$$p = \mu\left[n(t = 0) + \rho\right]. \tag{17}$$

For this special case p is a constant, independent of deformation and time. Finally, (15) and (3a, 3d) imply that $P_{3\alpha} = P_{\alpha 3}$ and this ensures the true stress is symmetric. The true stress tensor can be computed using $\boldsymbol{\tau} = \mathbf{P}\left(\mathbf{F}^{0\to t}\right)^{\mathrm{T}}$ and is

$$\begin{aligned} &\tau_{11} = \tau_{12} = \tau_{22} = \tau_{21} = 0, \\ &\tau_{3\alpha} = P_{3\alpha} = 2\left[n(t) + \rho\right] W'(H_0)\, w_{,\alpha} \\ &\quad + 2\bar{\gamma}_\infty \textstyle\int_0^t \phi_B\left(\frac{t-\tau}{t_B}\right) W'(H)\,\Delta w_{,\alpha}\, d\tau, \\ &\tau_{33} = P_{31} w_{,1} + P_{32} w_{,2} + P_{33} \end{aligned} \tag{18a–c}$$

The nominal stress P_{33} in (3b) can be simplified using (15) and is

$$P_{33} = -2\bar{\gamma}_\infty \int_0^t \phi_B \left(\frac{t-\tau}{t_B}\right) W'(H) \left[w_{,1}\,\Delta w_{,1} + w_{,2}\,\Delta w_{,2}\right] d\tau \tag{18d}$$

Note, in contrast to *linearized* anti-plane theory, *neither of the out of plane stress component* P_{33} *nor* τ_{33} *are zero*. Although this stress is completely determined by the shear stresses and the displacement gradient, they have *higher singularity* at the crack tip than the out of plane shear stresses because the displacement gradients are also singular there. Like the T stress in plane fracture, τ_{33} is parallel to the crack plane and in hyper-elastic crack problems, it has no effect on the energy release rate. However, the T stress is known to affect the stability of crack path (Cotterell and Rice 1980). Unlike the T stress, τ_{33} is highly singular and therefore in theory, could affect crack path in a significant way. If this hypothesis is correct, then the normal to the crack plane should rotate about the x_1 axis in Fig. 2. However, we are not aware of any literature that discuss this effect.

We end this section by noting that (9) and (14) imply that the partial differential equation (*PDE*) governing the displacement w is:

$$2\left[n(t)+\rho\right]\left[W'(H_0)\,w_{,\alpha}\right]_{,\alpha} + 2\bar{\gamma}_\infty \int_0^t \phi_B \left(\frac{t-\tau}{t_B}\right) \left(W'(H)\,\Delta w_{,\alpha}\right)_{,\alpha} d\tau = 0 \tag{19}$$

Note that (19) is *not* the general equation for anti-plane shear deformation since it uses the traction free boundary condition on the crack faces to determine f and d.

4 Results

In the following, we assume the specimen geometry and the manner of loading are consistent with anti-plane shear deformation. Although it is possible to consider multiple cracks, we assume a single traction free stationary crack occupying the interval $C = \{a \le x_1 \le b, x_2 = 0\}$. We allow a to be infinite, for example, $a = -\infty, b = 0$, corresponds to a semi-infinite crack. An example is shown in Fig. 2.

4.1 Relaxation test

Relaxation test is commonly used to study the mechanical behavior of rate dependent solids. In an *ideal* relaxation test, the boundary of the specimen is subjected to a fixed displacement *instantaneously*. For example, in the strip specimen shown in Fig. 2, this boundary condition is

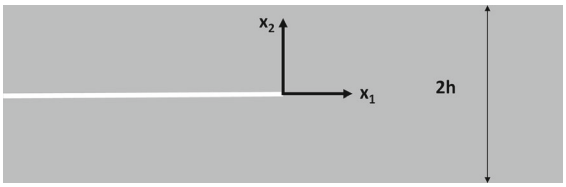

Fig. 2 The undeformed specimen consists of an infinite strip of height $2h$ with a semi-infinite crack. The strip is infinite in the x_1 and x_3 (out of plane) direction and is loaded by imposing equal and opposite out of plane displacement in the upper and lower faces

$$w(x_1, x_2 = \pm h, t \ge 0^+) = \pm w_0, \tag{20}$$

where w_0 is the imposed out of plane displacement. We seek a solution $w_E(\mathbf{x})$ in which the displacement in the cracked body is *independent of time*, i.e.,

$$w(x_1, x_2, t) = w_E(x_1, x_2) \tag{21}$$

This assumption implies that Δw in the integral in (19) is identically zero for all times. Thus, the governing equation for the displacement is:

$$\left[W'(H_0)\,w_{,\alpha}\right]_{,\alpha} = 0 \tag{22}$$

where $H_0 = 3 + w_{,\alpha}(\mathbf{x}) w_{,\alpha}(\mathbf{x})$. It is interesting to note that (22) is the governing equation of anti-plane deformation for a *hyper-elastic* solid with strain energy density function $W(I_1)$. Knowles (1977) and Rice (1967) have shown that the nonlinear PDE (22) can be transformed to a linear PDE using the Holograph transform. This fact allows us to establish the following correspondence principle for *relaxation* crack problems. That is, in a relaxation test, the displacement of the cracked body is independent of time and is identical to displacement w_E of an identical hyper-elastic cracked body with the same energy density function W. However, the true stresses are time dependent and decay with time according to:

$$\tau_{3\alpha} = P_{3\alpha} = 2\left[n(t)+\rho\right] W'\left(3 + w_{E,\beta}\, w_{E,\beta}\right) w_{E,\alpha} \equiv \left[n(t)+\rho\right] \tau_{E3\alpha} \tag{23a}$$

$$\tau_{33} = \left[n(t)+\rho\right]\left[\tau_{E31} w_{E,1} + \tau_{E32} w_{E,2}\right] \tag{23b}$$

where the subscript E in displacement and stress are used to indicate that these fields belong to the hyper-elastic solid. Thus, the stresses in the cracked body

behaves *like a hyper-elastic body where the shear modulus is multiplied by a decaying function of time.* Since $n(t \to \infty) = 0$, the cracked body relaxes to a hyper-elastic cracked body with reduced modulus $\mu\rho$ at long time. Physically, this stress relaxation corresponds to the breaking of physical bonds that are loaded at $t = 0^+$, *the integral term vanishes since physical bonds that are healed do not carry any load.*

As a concrete example, assume that the energy density function is given by

$$W(I_1) = \frac{\mu}{2B}\left\{\left[1 + \frac{B}{N}(I_1 - 3)\right]^N - 1\right\}, \tag{24}$$

where μ is the small strain shear modulus, $N > 1/2$ is a *strain hardening* parameter and $B > 0$ is a dimensionless material constant. The special case of $N = 1$ corresponds to a neo-Hookean solid; for this reason, this model is called the "Generalized neo-Hookean (GNH)" solid.

The asymptotic displacement w_E and the true tress field $\tau_{E3\alpha}$ near the crack tip for a GNH solid was obtained by Knowles (1977). With respect to a polar coordinate system (r, θ) in the *reference configuration*, they are

$$w_E \sim K r^m v(\theta) \quad m = 1 - \frac{1}{2N} \quad \theta \in [-\pi, \pi] \tag{25a}$$

$$\begin{aligned} \tau_{E3\alpha} &\sim \mu K^{2N-1}\left(\tfrac{B}{N}\right)^{N-1} \hat{\tau}_\alpha(\theta)\, r^{-(1-(1/2N))}, \\ \hat{\tau}_\alpha(\theta) &= \hat{h}^{N-1}(\theta)\left[\left(1 - \tfrac{1}{2N}\right) v(\theta)\, c_\alpha(\theta) \right. \\ &\quad \left. + \dot{v}(\theta)\, \varepsilon_{\beta\alpha} c_\beta(\theta)\right] \end{aligned} \tag{25b}$$

$$\tau_{E33} \sim \mu K^{2N}\left(\frac{B}{N}\right)^{N-1} \hat{h}^N(\theta)\, r^{-1} \tag{25c}$$

where $\dot{v}(\theta) = dv/d\theta$, $\varepsilon_{\beta\alpha}$ is the $2D$ alternator where $\varepsilon_{11} = \varepsilon_{22} = 0$, $\varepsilon_{12} = -\varepsilon_{21} = 1$ and

$$c_1(\theta) = \cos\theta,\ c_2(\theta) = \sin\theta \tag{25d}$$

$$v(\theta) = \sin(\theta/2)\left[\sqrt{1 - \frac{2(1 - 1/N)^2\cos^2(\theta/2)}{1 + \omega(\theta, N)}}\right]$$

$$[\omega(\theta, N) + (1 - 1/N)\cos\theta]^{\frac{N-1}{2N}} \tag{25e}$$

$$\omega(\theta, N) = \sqrt{1 - (1 - 1/N)^2 \sin^2\theta} \tag{25f}$$

$$\hat{h}(\theta) = \frac{(2N-1)^2}{4N^3}\left[(1 - 1/N)\cos\theta + \omega(\theta, N)\right]^{-1/N} \tag{25g}$$

Equations (25b, 25c) show that the stress field near the crack tip increases with strain hardening. Indeed, for very large N, all non-vanishing components of the true stress tensor are proportional to $1/r$. Also, as noted earlier, $\tau_{E33} \gg \tau_{E3\alpha}$ as $r \to 0$. Since all Mode III crack tip fields has the same functional form given by (25a–25c), K can be interpreted as an *intensity factor*. However, K cannot be determined by a local analysis since it depends on specimen geometry and the manner of loading. Knowles (1977) has shown that for *GNH* cracked bodies loaded under anti-plane shear, K is related to the path independent J integral by

$$\begin{aligned} A 2n K^{2N} &= \frac{B^{1-N} f_N}{\pi\mu} J, \\ f_N &= \frac{(4N^4)^N}{N(2N-1)^{2N-1}(2N^2 - 2N + 1)} \end{aligned} \tag{26}$$

An example where J can be obtained by elementary means is the strip sample shown in Fig. 2. Assuming that the upper and lower edges of the strip are subjected to a uniform displacement $\pm w_0$, translational invariance implies that

$$J = 2hW_\infty \tag{27}$$

where W_∞ is the strain energy density at $x_1 = \infty$ given by

$$W_\infty = \frac{\mu}{2B}\left\{\left[1 + \frac{B}{N}\left(\frac{w_0}{h}\right)^2\right]^N - 1\right\} \tag{28}$$

Substituting (28) into (27) and using (26) relates the intensity factor K to the applied displacement w_0, i.e.,

$$K^{2N} = \frac{hB^{-N} f_N}{\pi}\left\{\left[1 + \frac{B}{N}\left(\frac{w_0}{h}\right)^2\right]^N - 1\right\} \tag{29a}$$

For very large deformations where $w_0/h \gg 1$, (29a) is well approximated by

$$K = \left(\frac{hf_N}{\pi}\right)^{1/2N} \frac{1}{\sqrt{N}} \frac{w_0}{h} \tag{29b}$$

Since the local stresses is proportional to K^{2N-1} [see (25b, 25b)], (29b) implies that for large N the local stresses increase very rapidly with the imposed far field strain w_0/h.

For the special case of $N = 1$, the stresses are given by

$$\tau_{E31} \sim -\frac{\mu K}{2} r^{-1/2} \sin(\theta/2) \tag{30a}$$

$$\tau_{E32} \sim \frac{\mu K}{2} r^{-1/2} \cos(\theta/2) \tag{30b}$$

$$\tau_{E33} \sim \mu K^2 r^{-1}/4 \tag{30c}$$

where $K = \frac{2w_0}{\sqrt{\pi h}}$.

As is well known, the out of plane shear stresses $\tau_{E3\alpha}$ are identical to the *linearized* small strain anti-plane theory. For this case K is related to the Mode*III* stress intensity factor K_{III} by $K_{III} = \sqrt{\pi/2}\mu K$. A key difference between the linear and large deformation theory is that $\tau_{E33} = 0$ in the linearized theory whereas this is the dominant singularity in the nonlinear theory.

4.2 A special case: neo-Hookean

We are not aware of any analytical technique to obtain the general solution of (19) with arbitrary energy density function (see Sect. 4.3 for more details). However, the special case of Gaussian chains where W is neo-Hookean can be solved exactly. For this case, $W' = \mu/2$ and (19) reduces to

$$[n(t)+\rho]\, w_{,\alpha\alpha} + \bar{\gamma}_\infty \int_0^t \phi_B\left(\frac{t-\tau}{t_B}\right) (\Delta w_{,\alpha})_{,\alpha}\, d\tau = 0 \tag{31a}$$

Equation (31a) can be simplified by noting that the integral term is

$$\begin{aligned}
&\bar{\gamma}_\infty \int_0^t \phi_B\left(\frac{t-\tau}{t_B}\right) (\Delta w_{,\alpha})_{,\alpha}\, d\tau = \bar{\gamma}_\infty w_{,\alpha\alpha} \\
&(\mathbf{x}, t) \int_0^t \phi_B\left(\frac{t-\tau}{t_B}\right) d\tau - \bar{\gamma}_\infty \\
&\int_0^t \phi_B\left(\frac{t-\tau}{t_B}\right) w_{,\alpha\alpha}(\mathbf{x}, \tau)\, d\tau \\
&\quad = w_{,\alpha\alpha}(\mathbf{x}, t)\,[n_0 - n(t)] - \bar{\gamma}_\infty \\
&\int_0^t \phi_B\left(\frac{t-\tau}{t_B}\right) w_{,\alpha\alpha}(\mathbf{x}, \tau)\, d\tau
\end{aligned} \tag{31b}$$

where we have used (1c) and $n_0 \equiv n(t=0)$. Substituting (31b) into (31a), the governing PDE becomes:

$$(n_0+\rho)\, w_{,\alpha\alpha}(\mathbf{x}, t) - \bar{\gamma}_\infty \int_0^t \phi_B\left(\frac{t-\tau}{t_B}\right) w_{,\alpha\alpha}(\mathbf{x}, \tau)\, d\tau = 0 \tag{32}$$

Equation (32) is a linear Volterra integral equation of the second kind with a continuous kernel. It is well known that such equations has a unique solution (Kress 2014) which in this case is the trivial solution where

$$w_{,\alpha\alpha} = 0 \tag{33}$$

Thus, the displacement field satisfies the 2D Laplace equation, just as in the linearized small strain anti-plane shear theory. For the out of plane shear stresses, (18b) reduces to

$$\tau_{3\alpha} = P_{3\alpha} = \mu\,[n_0+\rho]\, w_{,\alpha}(\mathbf{x}, t) - \mu\bar{\gamma}_\infty \int_0^t \phi_B\left(\frac{t-\tau}{t_B}\right) w_{,\alpha}(\mathbf{x}, \tau)\, d\tau \tag{34a}$$

whereas

$$\begin{aligned}
\tau_{33} = {} & \mu\,[n_0+\rho]\,|\nabla w(\mathbf{x}, t)|^2 \\
& -2\mu\bar{\gamma}_\infty w_{,\alpha}(\mathbf{x}, t) \\
& \int_0^t \phi_B\left(\frac{t-\tau}{t_B}\right) w_{,\alpha}(\mathbf{x}, \tau)\, d\tau \\
& + \mu\bar{\gamma}_\infty \int_0^t \phi_B\left(\frac{t-\tau}{t_B}\right) |\nabla w(\mathbf{x}, \tau)|^2\, d\tau
\end{aligned} \tag{34b}$$

Correspondence principle

Equation (31a) can be written in a more suggestive form by defining a time dependent modulus

$$\mu_R(t) \equiv \mu\,[\rho + n(t)] \tag{35}$$

Integrating by parts and using (35) and (1c) shows that (31a) can be rewritten in the form of a linear viscoelastic model

$$\tau_{3\alpha} = P_{3\alpha} = \mu_R(t)\, w_{,\alpha}(\mathbf{x}, t=0) + \int_0^t \mu_R(t-\tau)\, \frac{\partial w_{,\alpha}(\mathbf{x}, \tau)}{\partial \tau} d\tau \tag{36}$$

where $\mu_R(t)$ is interpreted as the *shear relaxation function. Equation* (36) *implies that the usual correspondence principle of linear viscoelasticity applies to our model*. Two simple examples are:

(i) if traction boundary conditions are prescribed, then the stresses in the cracked body are the same as the stresses in an identically elastic cracked body ($\tau_{E3\alpha}$) subjected to the same traction (these stresses are independent of the shear modulus), and the displacement field can be obtained by inversion of (36) using Laplace transform, that is,

$$w_{,\alpha} = C(t)\,\tau_{E3\alpha}(\mathbf{x},0) + \int_0^t C(t-\tau)\,\frac{\partial \tau_{E3\alpha}(\mathbf{x},\tau)}{\partial \tau}d\tau \tag{37a}$$

where $C(t)$ is the creep function and is related to $\mu_R(t)$ by the convolution identity

$$\int_0^t \mu_R(t-\tau)\,C(\tau)\,d\tau = t. \tag{37b}$$

(ii) If a displacement boundary condition is prescribed on the cracked body (except on the traction free crack faces), then the displacement field is the same as the displacement of an identical neo-Hookean cracked body (w_E), which is independent of modulus, and the stresses can be found using (36). One can now use the large library of elastic crack solutions to solve a gel fracture problem.

For more general boundary conditions, the solution can be obtained using Laplace transform.

The correspondence principle implies that the displacement and shear stresses near the crack tip must have the form:

$$w \sim \frac{2K_{III}(t)}{\mu}\sqrt{r/2\pi}\,\sin(\theta/2)\;\; r \to 0 \tag{38a}$$

$$\begin{pmatrix}\tau_{31}\\ \tau_{32}\end{pmatrix} \sim \frac{K_{III}(t)}{\sqrt{2\pi r}}\begin{pmatrix}-\sin(\theta/2)\\ \cos(\theta/2)\end{pmatrix} \tag{38b,c}$$

where K_{III} is the Mode *III* stress intensity factor.

An example is a center crack of length $2a$ in an infinite block subjected to remote cyclic displacement of the form :

$$w(x_1, x_2 = \pm\infty, t) = \varepsilon_\infty x_2 \sin\omega t \tag{39}$$

The geometry is shown in Fig. 3. By the correspondence principle, the displacement field everywhere is

$$w(x_1,x_2,t) = (\varepsilon_\infty \sin\omega t)\,\mathrm{Im}\left[\sqrt{z^2-a^2}\right)\; where\; z = x_1 + ix_2 \tag{40}$$

where $i = \sqrt{-1}$. The crack opening displacement is

$$w\left(|x_1| \le a, x_2 = 0^{\pm}, t\right) = (\gamma_\infty \sin\omega t)\sqrt{a^2-x^2} \tag{41}$$

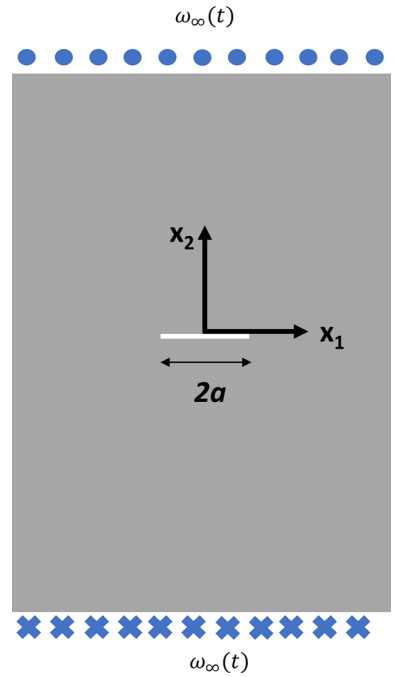

Fig. 3 An infinite block with a center crack 2a subject to remote cyclic displacement in Mode III

The shear stresses are

$$\tau_{32} + i\tau_{31} = \frac{\varepsilon_\infty}{\sqrt{1-a^2/z^2}}\int_0^t \mu_R(t-\tau)\,\frac{\partial \sin\omega\tau}{\partial\tau}d\tau \tag{42}$$

For very long times it is easy to show that the shear stresses approach a steady state given by

$$\tau_{32} + i\tau_{31} \to \tau_{32}^{ss} + i\tau_{31}^{ss} = \frac{\varepsilon_\infty}{\sqrt{1-a^2/z^2}}\left[\tilde{\mu}_R'(\omega)\sin\omega t + \tilde{\mu}_R''(\omega)\cos\omega t\right] \tag{43a}$$

where

$$\tilde{\mu}_R'(\omega) = \mu\rho + \mu\omega\int_0^\infty n(\eta)\sin\omega\eta d\eta = \mu\rho + \mu\bar{\gamma}_\infty\frac{t_B}{2-\alpha_B} - \mu\bar{\gamma}_\infty\frac{t_B}{\alpha_B-1}\int_0^\infty \cos\left(\frac{\omega t_B}{\alpha_B-1}x\right)(1+x)^{\frac{1}{1-\alpha_B}}dx, \tag{43b}$$

$$\tilde{\mu}_R''(\omega) = \mu\omega \int_0^\infty n(\eta)\cos\omega\eta d\eta = \mu\bar{\gamma}_\infty \frac{t_B}{\alpha_B - 1} \int_0^\infty \sin\left(\frac{\omega t_B}{\alpha_B - 1}x\right)(1+x)^{\frac{1}{1-\alpha_B}}\, dx \quad (43c)$$

are the storage and loss modulus respectively, and the second expressions of $\tilde{\mu}_R'(\omega)$ and $\tilde{\mu}_R''(\omega)$ are obtained by integration by parts and substituting the variable $x \equiv (\alpha_B - 1)\,\eta/t_B$. The long time modulus is given by $\mu\rho$. Because of dissipation caused by the breaking and reattaching of physical cross-links, the stresses are not in phase with the applied displacement.

4.3 Time dependent asymptotic crack tip fields

The difficulty with finding exact analytical solution with (19) is that

$$W'(H) = W'\left[3 + \Delta w_{,\alpha}(\mathbf{x},\tau,t)\,\Delta w_{,\alpha}(\mathbf{x},\tau,t)\right] \quad (44)$$

is a nonlinear function which depends on the *history* of the displacement. Because of this feature, the holograph transform does not work. Nevertheless, it is possible to obtain the asymptotic crack tip behavior for a wide class of energy density functions. For concreteness, we assume that the elasticity of the networks obey the GNH model. Knowles (1977) has shown that the displacement field near the crack tip has the form

$$w_E = Kr^m v(\theta),\ r \to 0 \quad m = 1 - \frac{1}{2N} \quad (45)$$

where K is a loading parameter and $v(\theta)$ is given by (25e). In our case we must allow the loading parameter K to be *time dependent*, which we indicate explicitly by $k(t)$, that is, we assume the crack tip displacement has the form:

$$w = k(t)\,r^m v(\theta) \equiv k(t)\chi(r,\theta),\ r \to 0 \quad (46)$$

where to simplify notation we denote $\chi(r,\theta) \equiv r^m v(\theta)$. Note that the GNH is locally homogeneous, in the sense that

$$W'[I_1 \to \infty] \approx \frac{\mu}{2}\left(\frac{B}{N}\right)^{N-1} I_1^{N-1} \quad N > 1 \quad (47)$$

The case of $N = 1$ corresponds to the neo-Hookean strain energy density function and was already considered above. The fact that $Kr^m \mathrm{v}(\theta)$ is the local solution of the elasticity problem means that

$$\left[W'(I_1)\,w_{E,\alpha}\right]_{,\alpha} \sim \frac{\mu}{2}\left(\frac{B}{N}\right)^{N-1} K\left[I_1^{N-1}\chi_{,\alpha}\right]_{,\alpha} \sim \frac{\mu}{2}\left(\frac{B}{N}\right)^{N-1} \left[K^{2N-1}\left(\chi_{,\beta}\chi_{,\beta}\right)^{N-1}\chi_{,\alpha}\right]_{,\alpha} \sim 0 \quad (48)$$

to *leading order as* $r \to 0$. Note the homogeneity of W' ensures that this result is valid irrespective of the value of K. Hence, by (46), the leading behavior of (2d) and (2f) at the crack tip is:

$$H_0(\mathbf{x} \to \mathbf{0}, t) \approx k^2(t)\left(\chi_{,\beta}\chi_{,\beta}\right), \quad (49a,b)$$
$$H(\mathbf{x} \to \mathbf{0}, \tau, t) \approx [k(t) - k(\tau)]^2\left(\chi_{,\beta}\chi_{,\beta}\right)$$

$$W'(H_0) \sim k^{2N-2}(t)\left(\chi_{,\beta}\chi_{,\beta}\right)^{N-1}, \quad (49c,d)$$
$$W'(H) \sim \left[k^2(t) - k^2(\tau)\right]^{2N-2}\left(\chi_{,\beta}\chi_{,\beta}\right)$$

Equations (48) and (49) imply that

$$\left[W'(H_0)\,w_{,\alpha}\right]_{,\alpha} \sim 0 \text{ and } \left[W'(H)\,w_{,\alpha}\right]_{,\alpha} \sim 0 \text{ as } r \to 0 \quad (50)$$

This means that (19) is satisfied to leading order as $r \to 0$, so the asymptotic displacement as $r \to 0$ must be given by (46). Of course, the function $k(t)$ cannot be determined by local analysis, it depends on loading history and geometry.

The near tip stresses are determined by substituting (46) into (18b,c) and keeping only the leading order terms, this results in

$$\tau_{3\alpha} \sim \mu\left(\frac{B}{N}\right)^{N-1} K_{\text{local}}(t/t_B)\, r^{-(1-(1/2N))}\hat{\tau}_\alpha(\theta) \quad (51a)$$

$$K_{\text{local}}(t/t_B) = [n(t) + \rho][k(t)]^{2N-1} + \bar{\gamma}_\infty \int_0^t \phi_B\left(\frac{t-\tau}{t_B}\right)[k(t) - k(\tau)]^{2N-1}\, d\tau \quad (51b)$$

The function $K_{\text{local}}(t/t_B)$ can be regarded as a *local intensity factor* since it carries all the loading information via $k(t)$. The asymptotic behavior of $\tau_{3\alpha}$ is determined by (46), (51a, 51b) and (18c).

Matched asymptotics: small scale hardening

In our fracture experiments using *plane stress* edge crack specimens, we find that the local crack opening displacements agree surprising well with the prediction of (1a) using the *neo-Hookean* energy density function (Guo et al. 2018). This suggests that strain hardening must be confined to a region Ω_{SH} near the crack tip that is very small in comparison with the

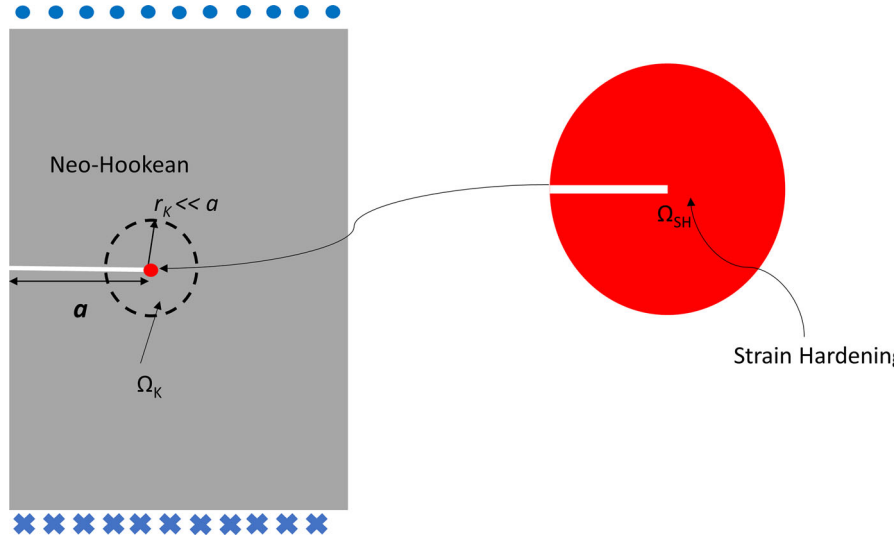

Fig. 4 Schematics of the small scale hardening

region of dominance of the stress field predicted using the neo-Hookean model, which we denote by Ω_K (see Fig. 4). Assuming that this is the case for a Mode III crack, we can link the near tip strain hardening behavior predicted by (51a, 51b) to the applied loading on a cracked body using a Small Scale Hardening (SSH) approach – a variation of the Small Scale Yielding approach in Elastic–Plastic Fracture (Zehnder 2012). In this approach, we use a boundary layer formulation where the physical crack is replaced by a semi-infinite traction free crack and the actual boundary conditions replaced by the neo-Hookean singular displacement at large distances in comparison with Ω_{SH}, as schematically shown in Fig. 4. In light of (34a), the *far field* boundary condition are:

$$w \to \frac{2K_{III}(t)}{\mu}\sqrt{r/2\pi}\,\sin(\theta/2) \text{ as } r \to \infty \tag{52}$$

where $K_{III}(t)$ is the time dependent stress intensity factor for the associated viscoelastic crack problem (with the neo-Hookean work function).

Equation (19) and dimensional analysis imply that the displacements must have the form:

$$w = \frac{K_{III}^2(t)}{\mu^2} D\left(\frac{r}{K_{III}^2(t)/\mu^2}, \theta, t/t_B, \bar{\gamma}_B t_B, B/N, \rho\right) \tag{53}$$

where D is a dimensionless function of its dimensionless arguments. Equation (46) implies that

$$\frac{K_{III}^2(t)}{\mu^2} D\left(\frac{r}{K_{III}^2(t)/\mu^2}, \theta, t/t_B, \bar{\gamma}_B t_B, B/N, \rho\right)$$

$$\to k(t)\, r^m v(\theta) \; r \to 0 \tag{54}$$

Equation (54) implies that

$$D\left(\frac{r}{K_{III}^2(t)/\mu^2}, \theta, t/t_B, \bar{\gamma}_B t_B, B/N, \rho\right)$$

$$\sim \left[\frac{r}{K_{III}^2(t)/\mu^2}\right]^m \psi(t)\, \mathrm{v}(\theta) \tag{55}$$

where ψ is some unknown function of time and is independent of $K_{III}^2(t)/\mu^2$. Comparison of (54) and (55) shows that

$$k(t) = \left[\frac{K_{III}^2(t)}{\mu^2}\right]^{1-m} \psi(t) \tag{56}$$

Substituting (56) into (51b) and using $1 - m = 1/2N$ gives:

$$K_{\text{local}}(t/t_B) = \Bigg[[n(t) + \rho]\,[\psi(t)]^{2N-1} + \bar{\gamma}_\infty$$

$$\int_0^t \phi_B\left(\frac{t-\tau}{t_B}\right)[\psi(t) - \psi(\tau)]^{2N-1}\, d\tau \Bigg]$$

$$\left[\frac{K_{III}(t)}{\mu}\right]^{\frac{2N-1}{N}} \tag{57}$$

Equation (57) connects the remote Mode III stress intensity factor $K_{III}(t)$ to the *local* stress intensity factor K_{local}. Unfortunately, the dimensionless function $\psi(t)$ can be determined only by solving (19) with the boundary condition (52). Finally, although we have

used the GNH energy density function in deriving the asymptotic fields and (57), there is nothing special about this model. For example, the same method can be applied to any energy density function as long as it is a function of I_1 and W' is locally homogeneous, that is:

$$W'[I_1 \to \infty] \approx I_1^{\beta}, \text{ for some positive power } \beta > 0 \tag{58}$$

5 Summary and discussion

In this work, we studied the near tip stress and strain fields of a Mode III crack in rate dependent hydrogels. We establish a global correspondence principle for the special case where the undamaged network obeys Gaussian statistics. We showed that the local time dependent asymptotic stress and strain fields have the same spatial dependence as the asymptotic stress and strain field of a hyper-elastic solid, as long as the energy density function is a function of I_1 only and W' is locally homogeneous. This result can be viewed as a *local correspondence principle* for the crack tip fields. We show that the near tip stress and strain fields are completely determined by a time dependent stress intensity factor $K_{\text{local}}(t)$. The local time dependent damage process near the crack tip is governed by the stress history. If we assume the region of local damage is sufficiently confined so that there exists a region near the crack tip where the stress field is completely determined by the local stress intensity factor $K_{\text{local}}(t)$, then the local strains and damage would have to be controlled by the history of $K_{\text{local}}(t)$. Hence $K_{\text{local}}(t)$ can be used as a history dependent loading parameter to determine when a pre-existing crack initiates growth. Note that since the material is rate dependent, whether a crack will grow or not depends on the entire time history $K_{\text{local}}(t)$, $0 \le t$ and not its current value alone. If the network energy density function is neo-Hookean, then the local stress intensity factor can be related to the remote loading history using classical theory of linear viscoelasticity via the correspondence principle, as shown in Sect. 4.2. For networks that do not obey Gaussian statistics, it is necessary to use the numerical method to determine the dependence of $K_{\text{local}}(t)$ on the loading history. Finally, this idea of using $K_{\text{local}}(t)$ as a criterion for crack initiation in principle should apply to plane stress and plane strain cracks, except in these cases the asymptotic behavior of the stress field near the crack tip is still to be determined. An interesting question is whether the local correspondence principle holds for cracks loaded under plane stress or plane strain conditions. We believe that it is possible to show that for plane stress or plane strain stationary crack problems, the asymptotic behavior of the integral term in Eq. (1a) as the crack tip is approached is either subdominant or has the same order of singularity as corresponding the nonlinear elastic solution. If this is true, the *spatial* variation of the near tip stress fields in our gel should be identical to a hyper-elastic solid in which the chains obey the same work function. We are currently working to prove this hypothesis.

Our analysis has several limitations. It assumes the crack is stationary and we have not proposed a local failure mechanism for the initiation of crack growth. This failure mechanism is still being studied. Here we note that the constitutive model cannot be applied to study failure, since we have assumed that the chains between chemical crosslinks cannot break. To study crack growth, we must relax this assumption to allow for chain breakage. Furthermore, it is reasonable to expect that crack growth can change the asymptotic behavior of the stress and strain fields near the crack tip, as is well known in elastic–plastic and elastic-power-law creeping materials (Chitaley and McClintock 1971; Hui and Riedel 1981). However, in slow crack growth, it is likely that these asymptotic fields for growing cracks are highly concentrated near the crack tip, and as a result, the asymptotic fields of the stationary crack may still control the crack growth process.

A different limitation of our analysis is that it is based on a constitutive model which is tested on a particular hydrogel ((PVA) dual crosslinked gel) and hence may not be applicable to other hydrogels with both chemical and transient bonds. However, our recent work (to be published) shows that, with some modification, our constitutive model can be used to characterize the mechanical properties of much tougher systems such as the polyampholyte hydrogel developed by Ihsan et al. (2016).

Acknowledgements The authors acknowledge support by the National Science Foundation under Grant No. CMMI -1537087.

References

Brown HR (2007) A model of the fracture of double network gels. Macromolecules 40:3815–3818

Chitaley AD, McClintock FA (1971) Elastic-plastic mechanics of steady crack growth under anti-plane shear. J Mech Phys Solids 19:147–163

Cotterell B, Rice JR (1980) Slightly curved or kinked cracks. Int J Fract 16:155–169

Gong JP (2010) Why are double network hydrogels so tough? Soft Matter 6:2583–2590

Gong JP, Katsuyama Y, Kurokawa T, Osada Y (2003) Double-network hydrogels with extremely high mechanical strength. Adv Mater 15:1155–1158

Guo J, Long R, Mayumi K, Hui C-Y (2016) Mechanics of a dual cross-link gel with dynamic bonds: steady state kinetics and large deformation effects. Macromolecules 49:3497–3507

Guo J, Liu M, Zehnder AT, Zhao J, Narita T, Creton C, Hui C-Y (2018) Fracture mechanics of a self-healing hydrogel with covalent and physical crosslinks: a numerical study. J Mech Phys Solids 120:79–95

Henderson KJ, Zhou TC, Otim KJ, Shull KR (2010) Ionically cross-linked triblock copolymer hydrogels with high strength. Macromolecules 43:6193–6201

Hui CY, Riedel H (1981) The asymptotic stress and strain field near the tip of a growing crack under creep conditions. Int J Fract 17:409–425

Ihsan AB, Sun TL, Kurokawa T, Karobi SN, Nakajima T, Nonoyama T, Roy CK, Luo F, Gong JP (2016) Self-healing behaviors of tough polyampholyte hydrogels. Macromolecules 49:4245–4252

Knowles JK (1977) The finite anti-plane shear field near the tip of a crack for a class of incompressible elastic solids. Int J Fract 13:611–639

Kress R (2014) Linear integral equations. Springer, New York

Kuo CK, Ma PX (2001) Ionically crosslinked alginate hydrogels as scaffolds for tissue engineering: part 1. Structure, gelation rate and mechanical properties. Biomaterials 22:511–521

Kwon HJ, Yasuda K, Gong JP, Ohmiya Y (2014) Polyelectrolyte hydrogels for replacement and regeneration of biological tissues. Macromol Res 22:227–235

Lee KY, Mooney DJ (2001) Hydrogels for tissue engineering. Chem Rev 101:1869–1880

Lin W-C, Fan W, Marcellan A, Hourdet D, Creton C (2010) Large strain and fracture properties of poly(dimethylacrylamide)/silica hybrid hydrogels. Macromolecules 43:2554–2563

Long R, Hui C-Y (2015) Crack tip fields in soft elastic solids subjected to large quasi-static deformation—a review. Extreme Mech Lett 4:131–155

Long R, Mayumi K, Creton C, Narita T, Hui C-Y (2014) Time dependent behavior of a dual cross-link self-healing gel: theory and experiments. Macromolecules 47:7243–7250

Long R, Mayumi K, Creton C, Narita T, Hui C-Y (2015) Rheology of a dual crosslink self-healing gel: theory and measurement using parallel-plate torsional rheometry. J Rheol 59:643–665

Mayumi K, Marcellan A, Ducouret G, Creton C, Narita T (2013) Stress–strain relationship of highly stretchable dual crosslink gels: separability of strain and time effect. ACS Macro Lett 2:1065–1068

Mayumi K, Guo J, Narita T, Hui CY, Creton C (2016) Fracture of dual crosslink gels with permanent and transient crosslinks. Extreme Mech Lett 6:52–59

Nakajima T, Kurokawa T, Ahmed S, Wu W, Gong JP (2013) Characterization of internal fracture process of double network hydrogels under uniaxial elongation. Soft Matter 9:1955–1966

Narita T, Mayumi K, Ducouret G, Hébraud P (2013) Viscoelastic properties of poly(vinyl alcohol) hydrogels having permanent and transient cross-links studied by microrheology, classical rheometry, and dynamic light scattering. Macromolecules 46:4174–4183

Qiu Y, Park K (2001) Environment-sensitive hydrogels for drug delivery. Adv Drug Deliv Rev 53:321–339

Rice J (1967) Stresses due to a sharp notch in a work-hardening elastic–plastic material loaded by longitudinal shear. J Appl Mech 34:287–298

Sun J-Y, Zhao X, Illeperuma WRK, Chaudhuri O, Oh KH, Mooney DJ, Vlassak JJ, Suo Z (2012) Highly stretchable and tough hydrogels. Nature 489:133–136

Sun TL, Kurokawa T, Kuroda S, Ihsan AB, Akasaki T, Sato K, Haque MA, Nakajima T, Gong JP (2013) Physical hydrogels composed of polyampholytes demonstrate high toughness and viscoelasticity. Nat Mater 12:932–937

Wang X, Hong W (2011) Pseudo-elasticity of a double network gel. Soft Matter 7:8576–8581

Webber RE, Creton C, Brown HR, Gong JP (2007) Large strain hysteresis and Mullins effect of tough double-network hydrogels. Macromolecules 40:2919–2927

Zehnder AT (2012) Fracture mechanics. Springer, Amsterdam